

Development of a Circularly Polarized HMSIW Antenna

Haozhan Tian* and Tatsuo Itoh

Abstract—A circularly polarized (CP) half-mode substrate integrated waveguide (HMSIW) cavity-backed antenna is developed by a novel design method in this paper. The single-fed antenna contains two coupled HMSIW cavities with orthogonal polarizations. Its design method evolves from filter synthesis procedure, which takes the advantage of equivalent circuit model to accelerate the optimization. The antenna radiates high-purity right handed CP waves with measured axial ratio (AR) of 0.33 dB at 3.55 GHz, while its gain and AR bandwidth are comparable to other CP SIW antennas. With the robust design method, the proposed antenna is competitive in practical applications.

1. INTRODUCTION

Antenna with circular polarization (CP) plays an important role in modern wireless communications. It solves the problem of the polarization mismatch caused by the multipath interference and the wave propagation in ionosphere. CP antenna with microstrip technology has been well studied, and the design procedure is mature [1–3]. However, microstrip antennas suffer from high conduction loss, which makes them less competitive in the high-frequency domain.

The substrate integrated waveguide (SIW) cavity-based CP antennas have low conduction loss and high gain, while maintaining the advantages of low profile, low cost, and easy integration with planar circuits [4–8]. However, generating pure CP waves in SIW cavities is not as straightforward as that in microstrip patches. The general solutions are either to design two standalone radiating elements [8], or to cut slots on top (or bottom) of the SIW cavity [4–7]. The first solution requires external feeding to provide the phase difference. For the second one, though widely used, the performance of the antennas is highly dependent on the shape, size, and location of the slots. Therefore, the design procedure typically involves heavy optimization in full-wave simulators, which takes a lot of time and computation.

In this paper, a CP antenna with SIW technique is developed by a fast and robust design methodology. The antenna contains two coupled half-mode SIW (HMSIW) cavities. The even and odd eigen-modes are excited inside the structure, similar to the coupled-mode patch antenna [9–11]. The design method evolves from filtering theory, where the equivalent circuit model is optimized to realize the target operating frequency and bandwidth. The final structure is directly synthesized from the circuit model, avoiding the heavy optimization in full-wave simulator. The proposed antenna has very low axial ratio (AR) at target frequency while still maintaining decent gain and AR bandwidth. The design procedures, along with the results and discussions, are presented in the following sections.

2. DESIGN METHOD AND THEORY

The schematic layout of the proposed antenna is shown in Fig. 1. Two identical HMSIW cavities have orthogonal polarization to each other. A gap on the center wall brings magnetic coupling between the

Received 6 August 2019, Accepted 10 September 2019, Scheduled 26 September 2019

* Corresponding author: Haozhan Tian (haozhan@g.ucla.edu).

The authors are with the Department of Electrical and Computer Engineering, University of California, Los Angeles, CA 90095, USA.

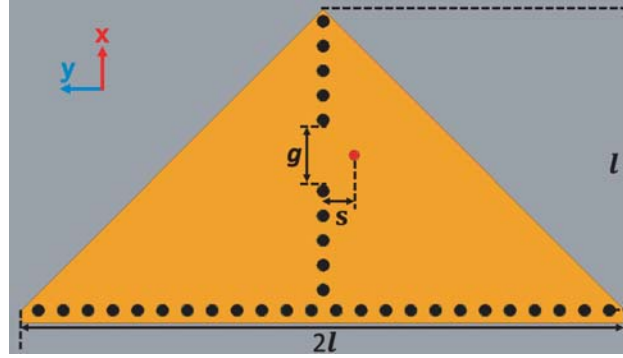


Figure 1. Top-view schematic layout of the proposed filtering antenna. The black dots represent the metal via posts connecting top to the ground, whose diameter is 1.6 mm and spacing is 3.2 mm. The red dot is the back-fed probe. The dimensions are all in mm: $l = 38.9$, $g = 7.5$, $s = 4$.

two cavities. Therefore, two eigen-modes, even and odd mode, can be supported. The antenna is back-fed through a coaxial cable to the right side cavity. The feeding breaks the symmetry of the excited modes, so that the radiating wave of the right HMSIW cavity leads the phase within the matching band [11]. As a result, RHCP is the co-polarization of the antenna. The antenna will radiate left handed CP (LHCP) waves if the feeding is symmetrically located to the left side. The design target is to have CP waves at center frequency of 3.58 GHz and achieve 3% impedance bandwidth. The substrate is a conductor-backed Rogers RT/duroid 5880 with dielectric constant of 2.2 and thickness of 1.57 mm. The design procedure and the theory are demonstrated in the following subsections.

2.1. Design Procedure

The first step is to build and characterize an HMSIW cavity resonant at target center frequency. The dimension of the cavity can be calculated by the equations [12]. The cavity is characterized by the equivalent circuit model as shown in Fig. 2. From the radiating edge to the left, it is a cavity resonator whose input admittance Y_c is modeled by shunt LC tank, L_c and C_c as show in Fig. 2(b). From the edge to the right side, the fringing field at the edge contributes to the additional capacitance of the cavity resonator and the radiation to the free space. The input admittance Y_r is thus modeled by shunt capacitance C_r and radiation conductance G_r . The values of the components in circuit model can be extracted based on the theoretical equations and HFSS simulator tool [13]. The impedance bandwidth of the whole antenna is limited by the quality factor of each HMSIW cavity, which can be calculated from the circuit model.

The second step is to construct and optimize the equivalent circuit model of the whole antenna

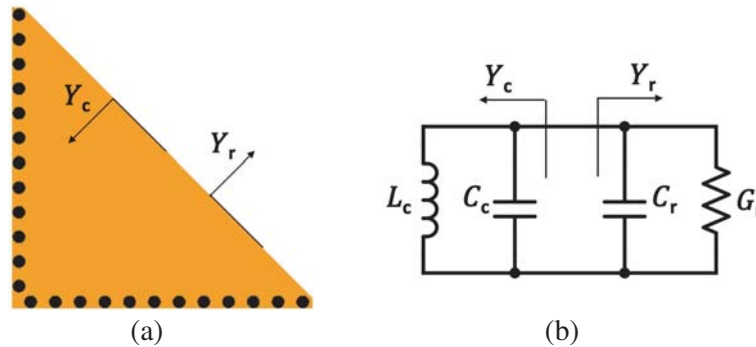


Figure 2. (a) HMSIW radiating resonator. (b) Equivalent lumped circuit model for the radiating resonator.

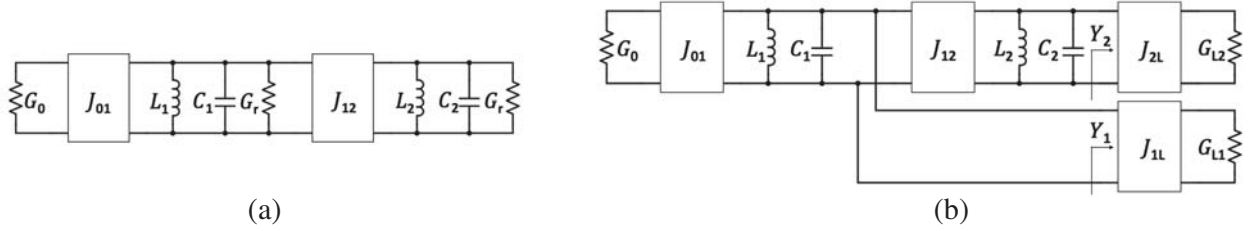


Figure 3. Equivalent circuit model loaded with (a) the radiation conductance G_r , and (b) the standard loads $G_{L1} = G_{L2} = 0.02$ S. The admittance inverters J_{1L} and J_{2L} are inserted in (b), such that $Y_1 = Y_2 = G_r$. The values are: $G_0 = 0.02$ S, $J_{01} = 1.29 \times 10^{-3}$ S, $J_{12} = 3.58 \times 10^{-4}$ S, $L_1 = L_2 = 0.42$ nH, $C_1 = C_2 = 4.71$ pF, $G_r = 2.98 \times 10^{-3}$ S, and $J_{1L} = J_{2L} = 1.07 \times 10^{-3}$ S.

as shown in Fig. 3. In Fig. 3(a), the two identical HMSIW radiating resonators are modeled by the way as discussed previously, where $C_1 = C_2 = C_c + C_r$. G_0 represents the source port, the admittance inverter J_{01} represents the external coupling, and J_{12} represents the internal coupling. In Fig. 3(b), the model translates the radiation conductance G_r to an inverter loaded by the standard load, where $Y_1 = Y_2 = G_r$. For both models, J_{01} and J_{12} are the only two variables that need to be determined.

The circuit model in Fig. 3(b) contains two independent loads, G_{L1} and G_{L2} , instead of one single load for regular filters. The two loads represent the radiation of the two HMSIW cavities with orthogonal polarization. The advantage of this model is to provide the delivered power ratio over the frequency. Since the antenna only has one single feed, the input power may not be equally delivered to the two orthogonal radiation loads. In order to get CP waves at target frequency, the three-port circuit prototype has to perform as a 3-dB power divider. Therefore, the internal and external coupling, J_{01} and J_{12} , are optimized to have the power equally divided at 3.58 GHz, and to achieve the desired bandwidth. For linear circuit model like the one in Fig. 3(b), the embedded optimizer in ADS can solve the problem efficiently and effectively.

Figure 4 shows the optimized results of the equivalent circuit model. S_{21} and S_{31} indicate the power ratio delivered to load G_{L1} and G_{L2} respectively, while S_{11} indicates the input matching. The target 10-dB fractional bandwidth of 3.0% at center frequency of 3.58 GHz is realized. The two nulls in S_{11} are at 3.55 GHz and 3.60 GHz. The input power is evenly delivered to the two loads at center frequency, since $S_{21} = S_{31} = -3$ dB. Away from the center frequency, more power is delivered to G_{L1} than that to G_{L2} , since the source feeds directly to Resonator 1.

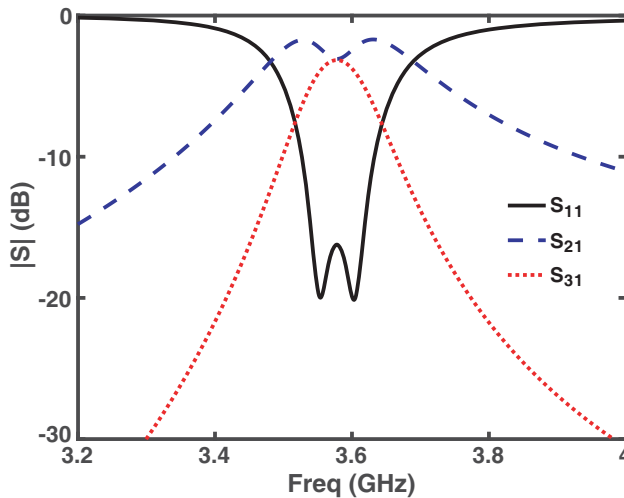


Figure 4. Frequency response of the circuit model shown in Fig. 3(b), where G_0 , G_{L1} , and G_{L2} refer to Port 1, 2, and 3 respectively.

The last step of the design procedure is to design the antenna based on the circuit model. In fact, only the gap in the center wall and the input feeding location need to be designed. Similar to a second-order SIW filter, the gap size is determined by the internal coupling coefficient k , and the feeding location is determined by the external quality factor Q_e . The values of k and Q_e can be derived from the circuit model by

$$Q_e = \frac{b_1 G_0}{J_{01}^2} \quad (1)$$

$$k = \frac{J_{12}}{\sqrt{b_1 b_2}} \quad (2)$$

where $b_i = 2\pi f_0 C_i$ for $i = 1, 2$ [14]. The gap size and feed location can then be realized with same design methods of resonator filters [15]. Once the gap and feeding are determined, the two orthogonally polarized HMSIW cavities will radiate out equal amount of energy as predicted by the circuit model. However, the circuit model cannot predict the phase difference between the two radiating edges. In the following subsection, we will analyze the eigen-modes and demonstrate that the phase difference is always 90° at the center frequency.

2.2. Mode Analysis

The even and odd eigen-modes are supported within the structure since the two HMSIW cavities are coupled through the gap in the center wall. Fig. 5 shows the distributions of the magnitude of E field and the vector of surface current density J at even and odd modes under eigen-mode simulation in HFSS. Half TM_{110} mode is supported in each HMSIW cavity resonator as shown in Figs. 5(a) and (b). The vector distributions of surface J in Fig. 5(c) are symmetric to the center wall, which indicates the even mode; while they are antisymmetric in Fig. 5(d), which indicates the odd mode. The fields along the two edges are in-phase at even mode and 180° out-of-phase at odd mode.

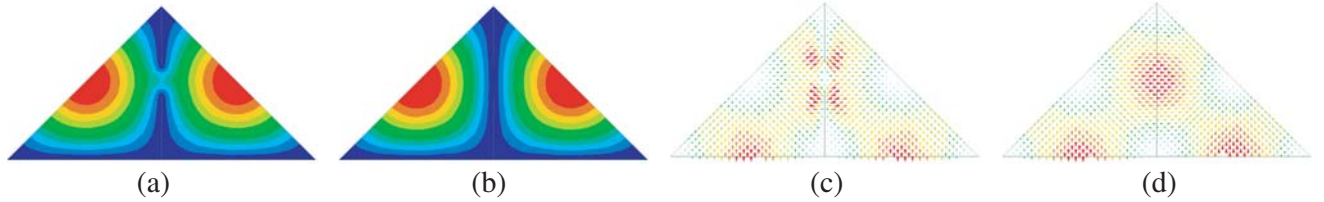


Figure 5. Simulated distributions of the complex E field magnitude at (a) even mode and (b) odd mode, and the surface J vector at (c) even mode and (d) odd mode.

The frequencies of the two modes are corresponding to the two nulls of S_{11} . The lower frequency null is the even mode while the higher one is odd mode, due to the magnetic coupling between the two HMSIW cavities. When the frequency increases from low to high null, the phase difference gradually changes from 0° to 180° . As a result, the phase difference will always be 90° at the center frequency. The input feeding will determine which side of the cavity leads the phase [11]. In our design, the right side cavity is directly fed through the coaxial cable and it then leads the phase. Therefore, the proposed antenna will radiate RHCP waves around the center frequency. Since the two cavities are symmetric, the antenna can be easily modified to radiate LHCP waves by moving the input feeding to the left side cavity. The full-wave simulation is demonstrated in Section 3 along with the measured results.

3. ANTENNA RESULTS

Figure 6 shows the simulated and measured S_{11} and broadside AR of the proposed antenna. The simulated S_{11} has 3.0% fractional bandwidth with center frequency at 3.58 GHz, identical to the circuit-model S_{11} . The measured S_{11} has 3.2% fractional bandwidth with center frequency at 3.55 GHz. The whole band slightly shifts to the lower frequency due to the fabrication tolerance. The measured two

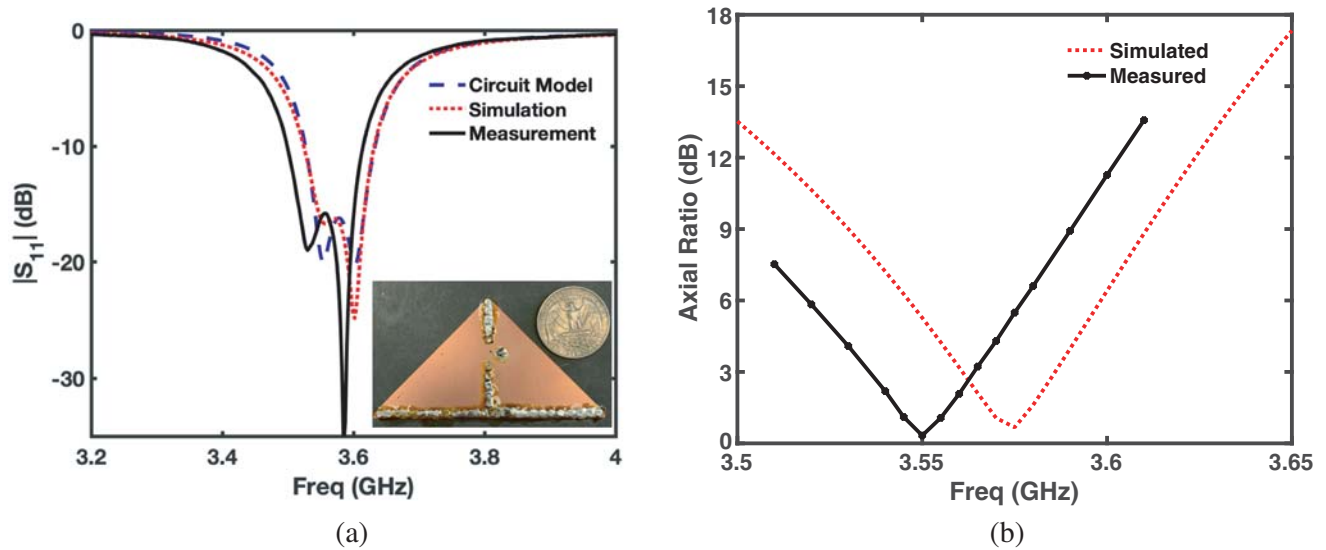


Figure 6. Simulated and measured (a) S_{11} response and (b) Axial Ratio (AR) of the proposed antenna at broadside. The inset figure in (a) shows the fabricated sample.

nulls are at 3.53 GHz and 3.59 GHz. The simulated broadside AR reaches its minimum of 0.67 dB at 3.58 GHz, as shown in Fig. 6(b). The 3-dB bandwidth of the simulated AR is 0.7%. The measured AR has the 3-dB bandwidth of 0.8% with the minimum of 0.33 dB at 3.55 GHz. The very low AR indicates that the CP waves are well-established by the proposed antenna. The measured and simulated AR closely resemble each other, though the frequency still shifts like S_{11} .

The surface-J distribution on the top metal of the structure at simulated center frequency is shown in Fig. 7(a). When the current of the right side HMSIW cavity reaches maximum, the current of the left side one is almost zero. This implies that the phase difference between the two radiating edges at the center is indeed 90° . Fig. 7(b) shows the radiation patterns of the proposed antenna on xz plane at center frequency. The simulated and measured results match well with each other. There is a null at broadside of the LHCP pattern, which indicates that the proposed antenna radiates pure RHCP waves there, consistent with the result of AR.

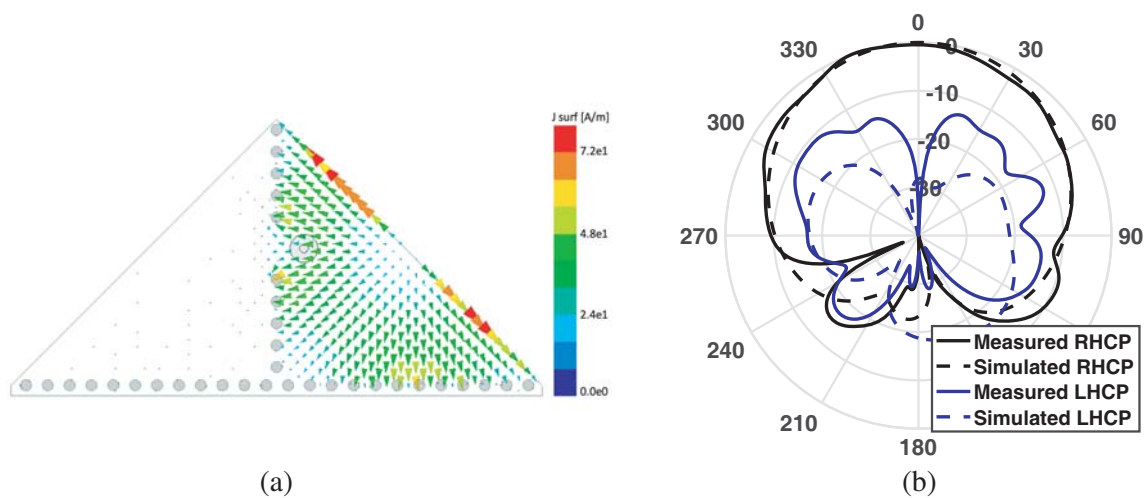


Figure 7. (a) Simulated distribution of surface J at center frequency. (b) Simulated and measured radiation patterns on xz plane at center frequency.

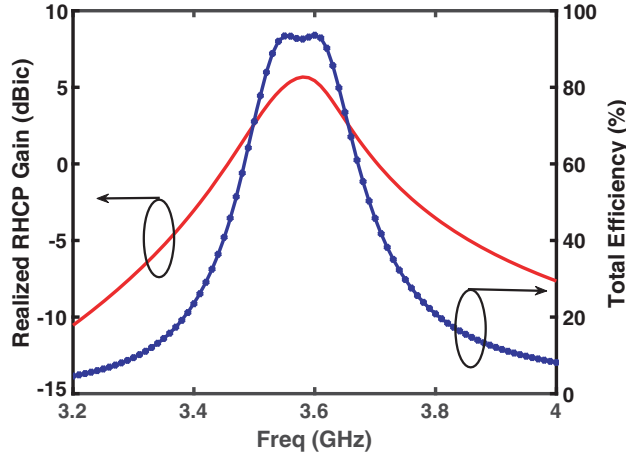


Figure 8. Simulated broadside realized gain of RHCP and total efficiency of the proposed antenna.

The simulated realized RHCP gain and the radiation efficiency of the proposed antenna are shown in Fig. 8. The realized gain and total efficiency discussed in this paper take the return loss into account. The peak gain of 5.7 dBic is realized at the center 3.58 GHz. The total radiation efficiency within the simulated matching band is around 90%, which indicates the low-loss feature of the HMSIW cavity-backed antenna. The two peaks of the total efficiency curve are corresponding to two matching nulls.

Table 1 compares the proposed design with other SIW-based CP antennas. The proposed antenna has the lowest AR, while maintaining comparable AR bandwidth and gain. In addition, the proposed design method of this antenna is fast and robust. The circuit simulator replaces the full-wave simulator for the design optimization to a large extent. As a result, the antenna can be efficiently designed for the specified frequency, impedance bandwidth, and substrate.

Table 1. Comparison of SIW based CP antennas.

| SIW CP Antennas | Freq (GHz) | Minimum AR (dB) | AR Bandwidth | Gain (dBic) |
|-----------------|------------|-----------------|--------------|-------------|
| This work | 3.55 | 0.33 | 0.80% | 5.7 |
| [4] | 10.1 | 1.1 | 0.8% | 6 |
| [5] | 8.75 | 1.15 | 0.66% | 5.12 |
| [6] | 10.2 | 1.3 | 2.35% | 6 |
| [7] | 28 | 1.2 | 2.25% | 5.3 |

4. CONCLUSION

A CP SIW-based antenna and its design procedure are demonstrated in this paper. The single-fed antenna contains two coupled HMSIW cavities with orthogonal polarizations. It has very low measured AR with decent gain and bandwidth. The design follows a novel circuit-model-based design procedure. A three-port equivalent circuit model is built and optimized to realize the target operating frequency and impedance bandwidth. During the design, the circuit simulator replaces the full-wave simulator to a large extent, which makes the procedure more efficient. The proposed CP SIW antenna with the design method is robust and competitive for practical applications.

REFERENCES

1. Balanis, C. A., *Antenna Theory: Analysis and Design*, John Wiley & Sons, 2016.
2. Yang, S. S., K.-F. Lee, A. A. Kishk, and K.-M. Luk, "Design and study of wideband single feed circularly polarized microstrip antennas," *Progress In Electromagnetics Research*, Vol. 80, 45–61, 2008.
3. Kasabegouadar, V. G. and K. J. Vinoy, "A broadband suspended microstrip antenna for circular polarization," *Progress In Electromagnetics Research*, Vol. 90, 353–368, 2009.
4. Luo, G. Q., Z. F. Hu, Y. Liang, L. Y. Yu, and L. L. Sun, "Development of low profile cavity backed crossed slot antennas for planar integration," *IEEE transactions on Antennas and Propagation*, Vol. 57, No. 10, 2972–2979, 2009.
5. Razavi, S. A. and M. H. Neshati, "Development of a low-profile circularly polarized cavity-backed antenna using HMSIW technique," *IEEE Transactions on Antennas and Propagation*, Vol. 61, No. 3, 1041–1047, 2012.
6. Kim, D. Y., J. W. Lee, T. K. Lee, and C. S. Cho, "Design of SIW cavity-backed circular-polarized antennas using two different feeding transitions," *IEEE Transactions on Antennas and Propagation*, Vol. 59, No. 4, 1398–1403, 2011.
7. Wu, Q., H. Wang, C. Yu, and W. Hong, "Low-profile circularly polarized cavity-backed antennas using SIW techniques," *IEEE Transactions on Antennas and Propagation*, Vol. 64, No. 7, 2832–2839, 2016.
8. Kim, K. and S. Lim, "Miniaturized circular polarized TE_{10} -mode substrate-integrated-waveguide antenna," *IEEE Antennas and Wireless Propagation Letters*, Vol. 13, 658–661, 2014.
9. Tian, H., K. Dhvaj, L. J. Jiang, and T. Itoh, "Beam scanning realized by coupled modes in a single-patch antenna," *IEEE Antennas and Wireless Propagation Letters*, Vol. 17, No. 6, 1077–1080, 2018.
10. Tian, H., L. J. Jiang, and T. Itoh, "A compact single-element pattern reconfigurable antenna with wide-angle scanning tuned by a single varactor," *Progress In Electromagnetics Research C*, Vol. 92, 137–150, 2019.
11. Tian, H., L. J. Jiang, and T. Itoh, "Compact endfire coupled-mode patch antenna with vertical polarization," *IEEE Transactions on Antennas and Propagation*, Vol. 67, No. 9, 5885–5891, 2019.
12. Pozar, D. M., *Microwave Engineering*, John Wiley & Sons, 2009.
13. Dhvaj, K., J. M. Kovitz, H. Tian, L. J. Jiang, and T. Itoh, "Half-mode cavity-based planar filtering antenna with controllable transmission zeroes," *IEEE Antennas and Wireless Propagation Letters*, Vol. 17, No. 5, 833–836, 2018.
14. Hong, J. S. G. and M. J. Lancaster, *Microstrip Filters for RF/Microwave Applications*, John Wiley & Sons, 2004.
15. Cameron, R. J., C. M. Kudsia, and R. R. Mansour, *Microwave Filters for Communication Systems: Fundamentals, Design, and Applications*, John Wiley & Sons, 2018.